Available online at www.sciencedirect.com

ScienceDirect

Journal of Computational and Applied Mathematics 215 (2008) 503–511

JOURNAL OF COMPUTATIONAL AND APPLIED MATHEMATICS

www.elsevier.com/locate/cam

Numerical modeling of free field vibrations due to pile driving using a dynamic soil-structure interaction formulation

H.R. Masoumi*, G. Degrande

Department of Civil Engineering, K.U. Leuven, Kasteelpark Arenberg 40,B-3001 Leuven, Belgium

Received 16 September 2005

Abstract

This paper presents a numerical model for the prediction of free field vibrations due to vibratory and impact pile driving. As the focus is on the response in the far field, where deformations are relatively small, a linear elastic constitutive behavior is assumed for the soil. The free field vibrations are calculated by means of a coupled FE–BE model using a subdomain formulation. The results show that, in the near field, the response of the soil is dominated by a vertically polarized shear wave, whereas in the far field, Rayleigh waves dominate the ground vibration and body waves are importantly attenuated. Finally, the computed ground vibrations are compared with the results of field measurements reported in the literature.

Keywords: Dynamic soil–pile interaction; Pile impedance; Vibratory pile driving; Impact pile driving; Ground vibration; Boundary element method; Finite element method

1. Introduction

Construction vibrations often affect adjacent and surrounding buildings in urban environments. The induced waves propagate in the soil and may interact with nearby structures, which induces vibrations that may cause cracks in its walls or in the facade. Permanent settlement, densification and liquefaction may also occur in the soil due to such vibrations. The present study aims to develop a model to predict free field vibrations in the environment due to pile driving. The vibration transmission through the soil is complex, as the soil behavior of the around the pile is difficult to describe. Ground motions due to pile driving generally depend on (1) the source parameters (method of driving, energy released, and pile depth), (2) the interaction between the driving machine, the pile and the soil, and (3) the propagation of the waves through the soil. Research on pile driving problems has concentrated on two main directions. Setting up numerous field measurements, several authors have focused on environmental effects (far field or external effects) [5,8]. Some efforts have been also made to develop models to assess the driving efficiency, investigating the driveability and the bearing capacity of driven piles (near field or internal effects) [7].

During pile driving, the transmitted energy through the soil is very high and causes plastic deformations in the near field. In the far field, however, reported data show that the induced vibrations cause deformations in the elastic

* Corresponding author.
E-mail address: hamidreza.masoumi@bwk.kuleuven.be (H.R. Masoumi).

0377-0427/$ - see front matter © 2007 Elsevier B.V. All rights reserved.
doi:10.1016/j.cam.2006.03.051

range [5]. As the focus is on the response in the far field, where deformations are relatively small, a linear elastic constitutive behavior is assumed for the soil.

In this study, a model for both vibratory and impact driving is proposed to predict free field vibrations. Using a subdomain formulation for dynamic soil-structure interaction, developed by Aubry et al. [1,2], the dynamic soil–pile interaction problem is investigated. A coupled FE–BE model is presented, in which the pile (bounded domain) and the soil (unbounded domain) are modeled using the finite element (FE) method and the boundary element (BE) technique, respectively. The subdomain formulation has been implemented in a computer program MISS (Modélisation d'Interaction Sol-Structure) [3]. The program MISS is used to determine the impedance functions and the modal responses of the soil in the frequency domain. The dynamic impedance of the soil is calculated by means of a boundary element formulation based on the Green's function of a horizontally stratified soil.

2. Numerical modeling

The proposed model is based on the following hypotheses: (1) the soil medium is elastic with frequency independent material damping (hysteresis damping), (2) no separation is allowed between the pile and soil medium, (3) all displacements and strains remain sufficiently small, and (4) the pile is embedded in a horizontally layered soil.

The domain is decomposed into two subdomains: the unbounded semi-infinite layered soil denoted by $\Omega_{\mathrm{s}}^{\mathrm{ext}}$ and the bounded structure (pile) denoted by Ω_{p}. The interface between the soil and the pile is denoted by Σ (Fig. 1a).

2.1. Governing equations

The deformations are assumed to be small enough to allow for a linear approximation of the constitutive equations, so that all equations can be elaborated in the frequency domain. The displacement wave fields in each subdomain during the dynamic excitation are denoted by $\mathbf{u}_\alpha(\mathbf{x}, \omega)$ where $\alpha = s$ denotes the soil and $\alpha = p$ refers to the pile. The stress tensors $\boldsymbol{\sigma}_\alpha(\mathbf{u}_\alpha)$ can be expressed as linear functions of the strain tensors $\boldsymbol{\epsilon}_\alpha(\mathbf{u}_\alpha)$ using Hooke's law:

$$\sigma_{\alpha ij} = \lambda_\alpha \varepsilon_{\alpha kk} \delta_{ij} + \mu_\alpha \varepsilon_{\alpha ij}, \tag{2.1}$$

where the components of the small strain tensor are calculated from the displacements as follows:

$$\varepsilon_{\alpha ij} = \tfrac{1}{2}(u_{\alpha i,j} + u_{\alpha j,i}), \tag{2.2}$$

where λ_α and μ_α are the Lamé parameters. In order to account for the dissipation of the internal energy in the soil (material damping), complex Lamé coefficients are used:

$$\mu_{\mathrm{s}}^* = \mu_{\mathrm{s}}(1 + 2i\beta_{\mathrm{s}}), \quad \lambda_{\mathrm{s}}^* = \lambda_{\mathrm{s}}(1 + 2i\beta_{\mathrm{s}}), \tag{2.3}$$

where β_{s} is the material damping ratio.

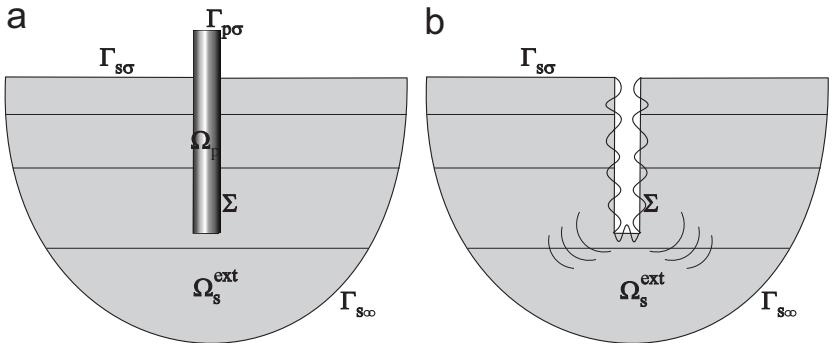

Fig. 1. (a) Geometry of the subdomains and (b) the scattered wave fields $\mathbf{u}_{\mathrm{sc}}(\mathbf{u}_{\mathrm{p}})$.

First, the pile Ω_p is considered. The boundary $\Gamma_p = \Gamma_{p\sigma} \cup \Sigma$ of the pile Ω_p is decomposed into a boundary $\Gamma_{p\sigma}$ where tractions $\bar{\mathbf{t}}_p$ are imposed and the soil–pile interface Σ. The displacement vector $\mathbf{u}_p$ of the pile satisfies the following Navier equation and boundary conditions:

$$\operatorname{div} \boldsymbol{\sigma}_p(\mathbf{u}_p) = -\rho_p \omega^2 \mathbf{u}_p \quad \text{in } \Omega_p, \tag{2.4}$$

$$\mathbf{t}_p(\mathbf{u}_p) = \bar{\mathbf{t}}_p \quad \text{on } \Gamma_{p\sigma}, \tag{2.5}$$

with $\mathbf{t}(\mathbf{u}) = \boldsymbol{\sigma}(\mathbf{u}) \cdot \mathbf{n}$ the traction vector on a boundary with a unit outward normal vector $\mathbf{n}$.

Second, the exterior soil domain Ω_s^{ext} is taken into consideration. The boundary $\Gamma_s^{ext} = \Gamma_{s\sigma} \cup \Gamma_{s\infty} \cup \Sigma$ of the soil domain Ω_s^{ext} is decomposed into the boundary $\Gamma_{s\sigma}$ where tractions are imposed, the outer boundary $\Gamma_{s\infty}$ where radiation conditions are imposed and the soil-structure interface Σ. A free boundary or zero tractions are assumed on $\Gamma_{s\sigma}$. The displacement vector $\mathbf{u}_s$ of the soil satisfies the Navier equation and the following boundary conditions:

$$\operatorname{div} \boldsymbol{\sigma}_s(\mathbf{u}_s) = -\rho_s \omega^2 \mathbf{u}_s \quad \text{in } \Omega_s^{ext}, \tag{2.6}$$

$$\mathbf{t}_s(\mathbf{u}_s) = \mathbf{0} \quad \text{on } \Gamma_{s\sigma}. \tag{2.7}$$

Displacement compatibility and stress equilibrium are imposed on the interface Σ:

$$\mathbf{u}_s = \mathbf{u}_p \quad \text{on } \Sigma, \tag{2.8}$$

$$\mathbf{t}_p(\mathbf{u}_p) + \mathbf{t}_s(\mathbf{u}_s) = \mathbf{0} \quad \text{on } \Sigma. \tag{2.9}$$

According to the compatibility condition (2.8), the displacement vector $\mathbf{u}_s$ is termed as the wave fields $\mathbf{u}_{sc}(\mathbf{u}_p)$ that are radiated in the soil due to the pile motion $\mathbf{u}_p$, imposed on the interface Σ (Fig. 1b):

$$\mathbf{u}_s = \mathbf{u}_{sc}(\mathbf{u}_p) \quad \text{in } \Omega_s^{ext}. \tag{2.10}$$

The wave field $\mathbf{u}_{sc}(\mathbf{u}_p)$, radiated in the soil, satisfies the elastodynamic equation in Ω_s^{ext} and the following boundary conditions (Fig. 1b):

$$\operatorname{div} \boldsymbol{\sigma}_s(\mathbf{u}_{sc}(\mathbf{u}_p)) = -\rho_s \omega^2 \mathbf{u}_{sc}(\mathbf{u}_p) \quad \text{in } \Omega_s^{ext}, \tag{2.11}$$

$$\mathbf{t}_s(\mathbf{u}_{sc}(\mathbf{u}_p)) = \mathbf{0} \quad \text{on } \Gamma_{s\sigma}, \tag{2.12}$$

$$\mathbf{u}_{sc}(\mathbf{u}_p) = \mathbf{u}_p \quad \text{on } \Sigma. \tag{2.13}$$

2.2. Variational formulation

The equation of motion of the dynamic soil–pile interaction problem can be formulated in a variational form for any virtual displacement field $\mathbf{v}$ imposed on the pile:

$$\int_{\Omega_p} \boldsymbol{\epsilon}(\mathbf{v}) : \boldsymbol{\sigma}_p(\mathbf{u}_p)\, d\Omega - \omega^2 \int_{\Omega_p} \mathbf{v} \cdot \rho_p \mathbf{u}_p\, d\Omega = \int_{\Gamma_{p\sigma}} \mathbf{v} \cdot \bar{\mathbf{t}}_p\, d\Gamma + \int_{\Sigma} \mathbf{v} \cdot \mathbf{t}_p(\mathbf{u}_p)\, d\Sigma, \tag{2.14}$$

where : denotes the contraction of two tensors.

Accounting for the equilibrium on the soil–pile interface Σ in Eq. (2.9), the variational Eq. (2.14) becomes:

$$\int_{\Omega_p} \boldsymbol{\epsilon}(\mathbf{v}) : \boldsymbol{\sigma}_p(\mathbf{u}_p)\, d\Omega - \omega^2 \int_{\Omega_p} \mathbf{v} \cdot \rho_p \mathbf{u}_p\, d\Omega + \int_{\Sigma} \mathbf{v} \cdot \mathbf{t}_s(\mathbf{u}_{sc}(\mathbf{u}_p))\, d\Sigma = \int_{\Gamma_{p\sigma}} \mathbf{v} \cdot \bar{\mathbf{t}}_p\, d\Gamma. \tag{2.15}$$

A modal reduction technique is applied where an approximate solution is sought in a subspace of finite dimension. The pile displacement vector $\mathbf{u}_p$ is decomposed as a linear combination of vibration modes $\boldsymbol{\psi}_m (m = 1, \ldots, q)$:

$$\mathbf{u}_p \simeq \sum_{m=1}^{q} \boldsymbol{\psi}_m \alpha_m = \boldsymbol{\Psi} \boldsymbol{\alpha}, \tag{2.16}$$

where the modes $\boldsymbol{\psi}_m (m = 1, \ldots, q)$ are collected in a matrix $\boldsymbol{\Psi}$ and the modal coordinates $\alpha_m (m = 1, \ldots, q)$ are collected in a vector $\boldsymbol{\alpha}$. Several alternatives are possible for the selection of the modes $\boldsymbol{\psi}_m$ to describe the kinematics of the pile. In a Galerkin formulation, a similar modal decomposition is used for the vector $\mathbf{v}$ of virtual displacements:

$$\mathbf{v} = \sum_{m=1}^{q} \boldsymbol{\psi}_m \delta\alpha_m = \boldsymbol{\Psi}\boldsymbol{\delta\alpha}, \tag{2.17}$$

where $\boldsymbol{\delta\alpha}$ is a vector with virtual modal coordinates. Introducing the decompositions (2.16) and (2.17) in the virtual work expression (2.15) and expressing that the resulting equation must hold for any set of virtual modal coordinates $\boldsymbol{\delta\alpha}$ results into the following q-dimensional system of equations:

$$\left[\int_{\Omega_\mathrm{p}} \boldsymbol{\epsilon}(\boldsymbol{\Psi}) : \boldsymbol{\sigma}_\mathrm{p}(\boldsymbol{\Psi})\,\mathrm{d}\Omega - \omega^2 \int_{\Omega_\mathrm{p}} \boldsymbol{\Psi}^\mathrm{T}\rho_\mathrm{p}\boldsymbol{\Psi}\,\mathrm{d}\Omega + \int_{\Sigma} \boldsymbol{\Psi}^\mathrm{T}\mathbf{t}_\mathrm{s}(\mathbf{u}_\mathrm{sc}(\boldsymbol{\Psi}))\,\mathrm{d}\Sigma\right]\boldsymbol{\alpha} = \int_{\Gamma_{\mathrm{p}\sigma}} \boldsymbol{\Psi}^\mathrm{T}\bar{\mathbf{t}}_\mathrm{p}\,\mathrm{d}\Gamma. \tag{2.18}$$

2.3. Discretization of the variational formulation

In a FE formulation, the displacement field $\mathbf{u}_\mathrm{p}$ is approximated as $\mathbf{u}_\mathrm{p} \simeq \mathbf{N}_\mathrm{p}\underline{\mathbf{u}}_\mathrm{p}$, where $\mathbf{N}_\mathrm{p}$ are the globally defined shape functions and $\underline{\mathbf{u}}_\mathrm{p}$ is the displacement vector at all nodal points. Analogously, the strain vector $\boldsymbol{\epsilon}_\mathrm{p}$ is approximated as $\boldsymbol{\epsilon}_\mathrm{p} = \mathbf{L}\mathbf{N}_\mathrm{p}\underline{\mathbf{u}}_\mathrm{p} = \mathbf{B}_\mathrm{p}\underline{\mathbf{u}}_\mathrm{p}$, with $\mathbf{L}$ the matrix with derivative operators. The stress vector is defined as $\boldsymbol{\sigma}_\mathrm{p} = \mathbf{D}_\mathrm{p}\boldsymbol{\epsilon}_\mathrm{p}$, with $\mathbf{D}_\mathrm{p}$ the constitutive matrix for an isotropic linear elastic material.

Applying the same FE approximation to the modes of the pile $\boldsymbol{\psi}_m \simeq \mathbf{N}_\mathrm{p}\underline{\boldsymbol{\psi}}_m$, the modal decomposition (2.16) of the pile displacement vector can be written as follows:

$$\mathbf{u}_\mathrm{p} \simeq \mathbf{N}_\mathrm{p}\underline{\mathbf{u}}_\mathrm{p} \simeq \sum_{m=1}^{q} \mathbf{N}_\mathrm{p}\underline{\boldsymbol{\psi}}_m\alpha_m = \mathbf{N}_\mathrm{p}\underline{\boldsymbol{\Psi}}\boldsymbol{\alpha}. \tag{2.19}$$

Introducing this discretization into the system of equations (2.18) results in the following system of discretized equations, neglecting the effect of material damping in the pile:

$$\underline{\boldsymbol{\Psi}}^\mathrm{T}[\mathbf{K}_\mathrm{p} - \omega^2\mathbf{M}_\mathrm{p} + \mathbf{K}_\mathrm{s}]\underline{\boldsymbol{\Psi}}\boldsymbol{\alpha} = \underline{\boldsymbol{\Psi}}^\mathrm{T}\mathbf{f}_\mathrm{p}, \tag{2.20}$$

where the stiffness matrix $\mathbf{K}_\mathrm{p}$ and the mass matrix $\mathbf{M}_\mathrm{p}$ of the pile are defined as

$$\mathbf{K}_\mathrm{p} = \int_{\Omega_\mathrm{p}} \mathbf{B}_\mathrm{p}^\mathrm{T}\mathbf{D}_\mathrm{p}\mathbf{B}_\mathrm{p}\,\mathrm{d}\Omega, \quad \mathbf{M}_\mathrm{p} = \int_{\Omega_\mathrm{p}} \mathbf{N}_\mathrm{p}^\mathrm{T}\rho_\mathrm{p}\mathbf{N}_\mathrm{p}\,\mathrm{d}\Omega \tag{2.21}$$

and the vector of external forces $\mathbf{f}_\mathrm{p}$ on the pile is defined as

$$\mathbf{f}_\mathrm{p} = \int_{\Gamma_{\mathrm{p}\sigma}} \mathbf{N}_\mathrm{p}^\mathrm{T}\bar{\mathbf{t}}_\mathrm{p}\,\mathrm{d}\Gamma. \tag{2.22}$$

The dynamic stiffness matrix or impedance matrix $\mathbf{K}_\mathrm{s}$ of the semi-infinite layered soil domain $\Omega_\mathrm{s}^\mathrm{ext}$ around the pile is equal to

$$\mathbf{K}_\mathrm{s} = \int_{\Sigma} \mathbf{N}_\mathrm{p}^\mathrm{T}\mathbf{t}_\mathrm{s}(\mathbf{u}_\mathrm{sc}(\mathbf{N}_\mathrm{p}))\,\mathrm{d}\Sigma, \tag{2.23}$$

although it is preferable to compute directly its projection on the imposed displacement fields $\underline{\boldsymbol{\Psi}}$ of the pile:

$$\underline{\boldsymbol{\Psi}}^\mathrm{T}\mathbf{K}_\mathrm{s}\underline{\boldsymbol{\Psi}} = \int_{\Sigma} (\mathbf{N}_\mathrm{p}\underline{\boldsymbol{\Psi}})^\mathrm{T}\mathbf{t}_\mathrm{s}(\mathbf{u}_\mathrm{sc}(\mathbf{N}_\mathrm{p}\underline{\boldsymbol{\Psi}}))\,\mathrm{d}\Sigma. \tag{2.24}$$

This impedance matrix is calculated using a boundary element technique. As the BE method is based on the Green's functions of a horizontally layered half space, only a discretization of the interface Σ between the soil and the pile is required and the number of the unknowns is drastically reduced.

A computation procedure is developed to solve the governing system of equations (2.20). This procedure can be partitioned into two parts. First, using the Structural Dynamics Toolbox in MATLAB, the finite element model of the pile is made. In the second part, using the program MISS, the soil impedance $\underline{\boldsymbol{\Psi}}^{\mathrm{T}}\mathbf{K}_{\mathrm{s}}\underline{\boldsymbol{\Psi}}$ as well as the modal responses of the soil $\mathbf{u}_{\mathrm{sc}}(\boldsymbol{\Psi})$ are computed. The solution of the dynamic soil–pile interaction problem in terms of the modal coordinates allows to compute the soil tractions on the interface and, subsequently, in the free field.

3. Numerical example

The free field vibrations due to driving of a concrete pile in a semi-infinite medium are investigated. The pile has a length $L_{\mathrm{p}} = 10,$ m, a diameter $d_{\mathrm{p}} = 0.50$ m, a Young's modulus $E_{\mathrm{p}} = 40\,000$ MPa, a Poisson's ratio $\nu_{\mathrm{p}} = 0.25$, and a density $\rho_{\mathrm{p}} = 2500\,\mathrm{kg/m^3}$. The longitudinal wave velocity of the pile $C_{\mathrm{p}} = 4000$ m/s. The contributions of different types of waves are investigated for several penetration depths $e_{\mathrm{p}} = 2$, 5 and 10 m (Fig. 2).

The pile is modeled using 8-node isoparametric brick elements. Only the axial modes of the pile are excited due to vertical pile driving and considered in the modal superposition. The number of required modes depends upon the frequency content of the dynamic force. Fig. 3 shows the flexible modes of the pile with free boundary conditions. The first axial mode at 200.0 Hz corresponds to the first compression-tension mode.

The soil consists of a homogeneous half space with a Young's modulus $E_{\mathrm{s}} = 80$ MPa, a Poisson's ratio $\nu_{\mathrm{s}} = 0.4$, a material damping ratio $\beta_{\mathrm{s}} = 0.025$ and a density $\rho_{\mathrm{s}} = 2000\,\mathrm{kg/m^3}$. The shear wave velocity of the half space is

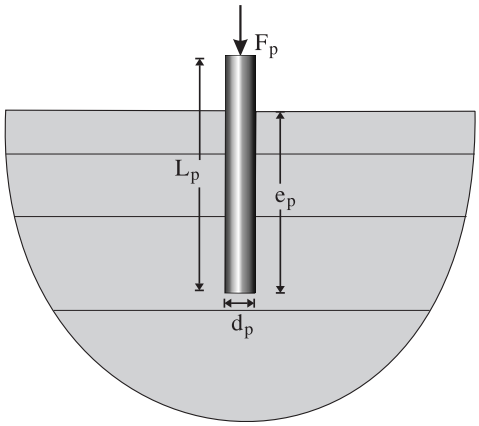

Fig. 2. Geometry of the problem.

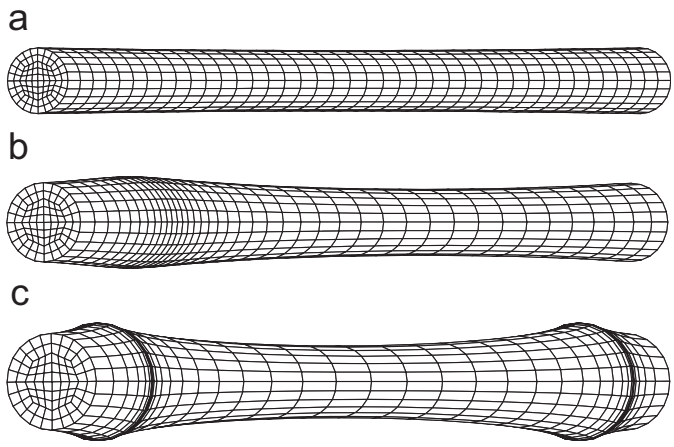

Fig. 3. First three flexible axial modes of the pile with free boundary conditions at (a) 200.0 Hz, (b) 400.3 Hz, and (c) 601.1 Hz.

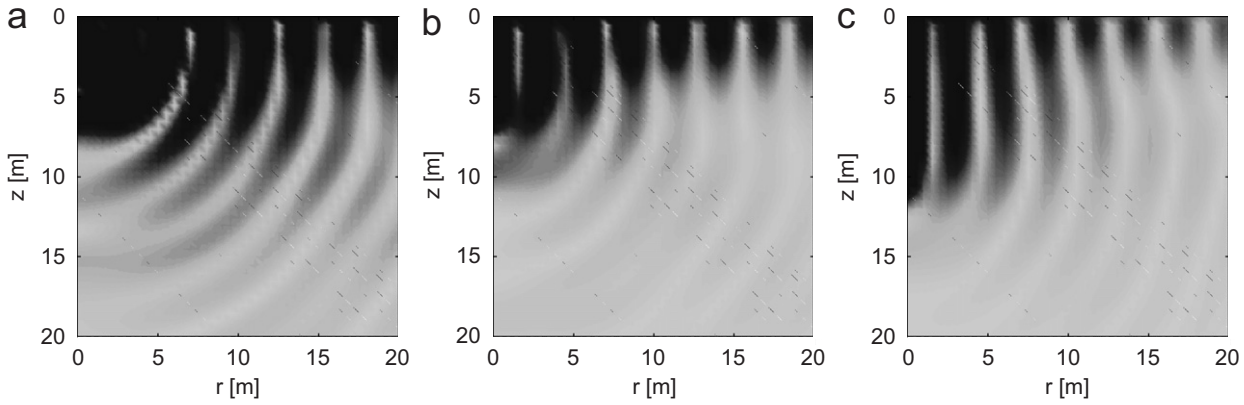

Fig. 4. The norm of the particle velocity in a homogeneous half space due to vibratory pile driving at 20 Hz for penetration depths (a) $e_p = 2$ m, (b) $e_p = 5$ m, and (c) $e_p = 10$ m.

$C_s = 120$ m/s.The size of each boundary element should be sufficiently small with respect to the minimum wavelength $\lambda_{min} = C_s/f_{max}$, where C_s is the shear wave velocity in the soil and f_{max} is the highest frequency in the dynamic excitation. It is proposed that the element size should be smaller than $\lambda_{min}/8$.

3.1. Ground vibrations due to vibratory pile driving

First, ground vibrations due to vibratory driving are considered. A standard hydraulic vibratory driver ICE 44-30V is selected. It operates at the frequency $f = 20$ Hz with an eccentric moment $me = 50.7$ kgm, resulting in a centrifugal force $F_p = 800$ kN. The results are presented in the (r, z) plane, where the vertical coordinate varies from $z = 0.0$ m at the ground surface to $z = 20$ m. The horizontal coordinate varies from the pile shaft at $r = 0.50$ m up to a distance $r = 20.5$ m from the pile center.

Fig. 4 shows the norm of the particle velocity due to vibratory pile driving at 20 Hz for different penetration depths $e_p = 2$, 5 and 10 m. The characteristics of the propagating waves induced by vibratory driving can be classified as follows: (1) because of the soil-shaft contact, vertically polarized shear waves are generated which propagate radially from the shaft on a cylindrical surface; (2) at the pile toe, shear and compression waves propagate in all directions from the toe on a spherical wave front; (3) Rayleigh waves propagate radially on a cylindrical wave front along the surface. When the pile toe is near the surface, ground motions are influenced only by toe resistance, and the response of the soil around the pile shaft is dominated by Rayleigh waves. As the pile is driven, the contact area along the pile shaft increases, and vertically shear waves dominate the response around the pile shaft. Fig. 4 shows how Rayleigh waves attenuate slower than body waves and propagate in a restricted zone close to the surface of the half space.

Fig. 5 illustrates the decrease of the peak particle velocity (PPV) at the surface with the distance r from the pile for three penetration depths $e_p = 2$, 5 and 10 m. The dashed-dotted line on the figure represents data obtained by several field measurements during vibratory pile driving [8]. The slope of the attenuation curve can be interpreted as an attenuation coefficient that represents the effect of both damping mechanisms. The numerical predictions reveal a larger attenuation coefficient for distances larger than 15 m, which may be attributed to the increased relative importance of material damping. The present model predicts higher ground vibrations in the far field, especially when the penetration depth is small. This may reflect the fact that during vibratory pile driving, higher (plastic) strains are induced in the soil, leading to more material damping [5].

3.2. Ground vibration induced by impact driving

Ground vibrations due to impact driving are subsequently investigated. A BSP-357 hammer is used to drive a concrete pile with the same characteristics as in the previous example.

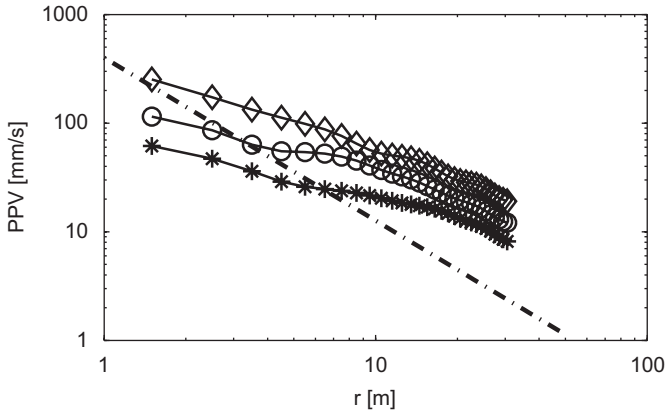

Fig. 5. PPV versus the distance from the pile due to vibratory pile driving at 20 Hz. Results obtained for the penetration depths $e_p = 2\,\text{m}$ ($-\diamond-$), $e_p = 5\,\text{m}$ ($-\circ-$), and $e_p = 10\,\text{m}$ ($-*-$) are compared with results of field measurements (dashed-dotted line) [8].

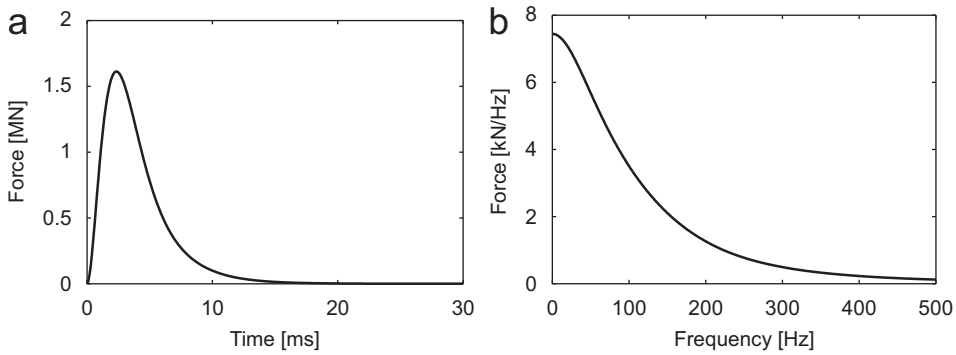

Fig. 6. (a) Time history and (b) frequency content of the impact force of a hammer with an impact velocity $v_0 = 1\,\text{m/s}$.

Fig. 6 shows the time history and frequency content of the hammer impact force. The force is evaluated using a 2DOF model developed in [4]. The hammer cushion is a steel plate with a stiffness $k_c = 1.6 \times 10^6\,\text{kN/m}$. The ram and anvil masses of the hammer are $m_r = 6860\,\text{kg}$ and $m_a = 850\,\text{kg}$, respectively. The pile impedance is equal to $Z_p = 1960\,\text{kNs/m}$.

In order to obtain an accurate inverse Fourier transform of the response from the frequency domain to the time domain, the frequency step Δf must be sufficiently small with respect to $C_R/r_{\max}$, where $r_{\max}$ represents the largest considered distance from the pile axis.

The boundary element analysis applied for the computation of the soil's impedance of structures embedded in the soil may suffer from the appearance of fictitious eigenfrequencies. For vibratory pile driving, the frequency of excitation is low, between 10 and 50 Hz, and fictitious eigenfrequencies are usually not a matter of concern. For impact driving, however, the frequency content of the loading is higher and fictitious frequencies need to be mitigated. A solution technique for elastodynamic problems has been proposed in [6], by analogy with Burton and Miller's approach for acoustic problems.

Fig. 7 shows the norm of the particle velocity in a homogeneous half space due to impact driving at different time steps $t = 30$, 80 and 160 ms and for different penetration depths. The following observations can be made: (1) body waves dominate around the toe and propagate on a spherical wave front; (2) vertically shear waves dominate around the pile and propagate radially on a cylindrical wave front; and (3) Rayleigh waves propagate near the surface with a velocity slightly less than shear waves.

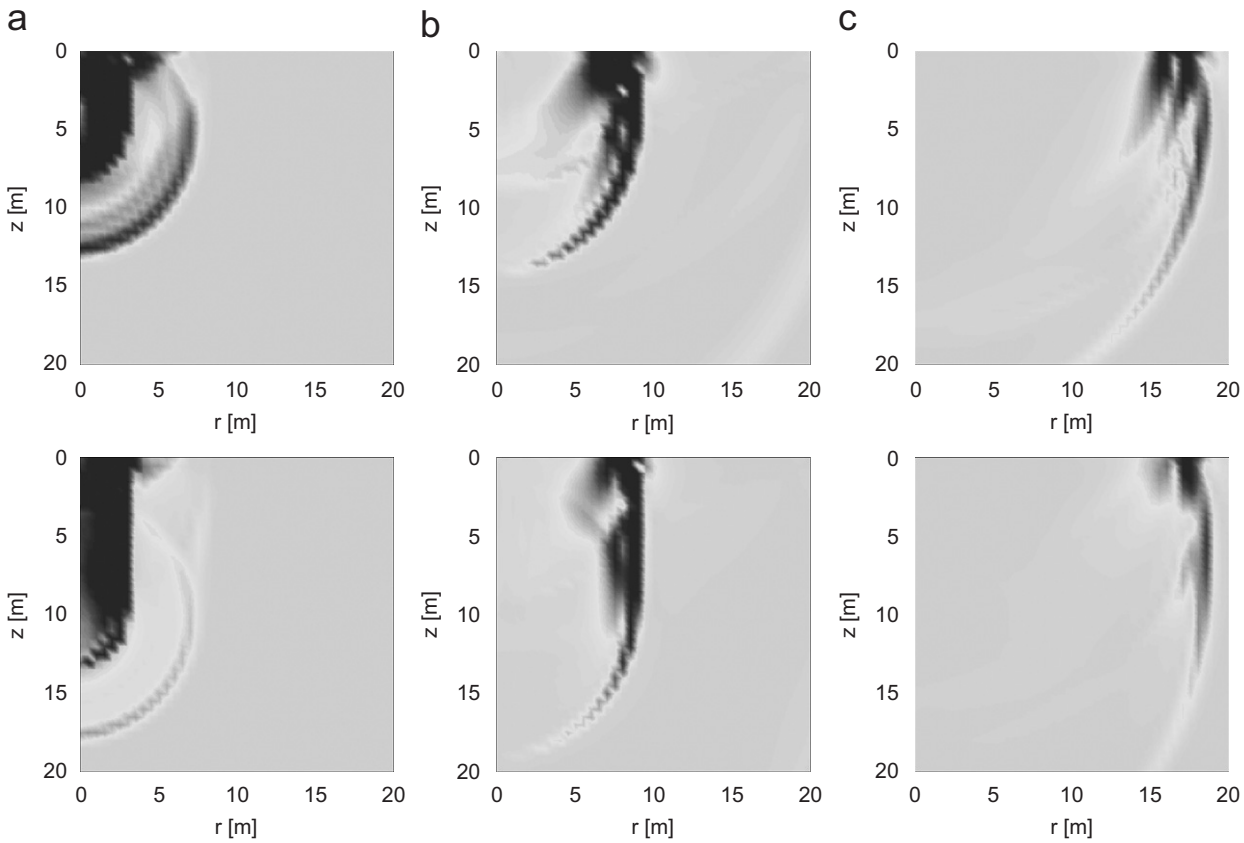

Fig. 7. The norm of the particle velocity in a homogeneous half space due to impact pile driving at time steps (a) $t = 30$ ms, (b) $t = 80$ ms, and (c) $t = 160$ ms for different penetration depths $e_p = 5.0$ m and 10.0 m.

4. Conclusions

A coupled FE–BE model has been developed to predict ground vibrations due to vibratory and impact pile driving. Using a subdomain formulation, a linear model for dynamic soil–pile interaction has been implemented. The pile is modeled using the finite element method. The soil is modeled as a horizontally layered elastic half space using a boundary element method.

The characteristics of the propagating waves around the pile have been investigated. In the case of vibratory driving, the induced waves can be classified into: (1) the vertically polarized shear waves around the shaft; (2) the body waves around the pile toe, and (3) the Rayleigh waves on the surface. Propagating waves due to impact driving are more complex. It is observed that deformations around the shaft are dominated by the vertically shear deformation where the normal and the radial deformations are small compared to shear deformations. In the far field, however, body waves are attenuated and Rayleigh waves dominate the zone near the surface, independent of the penetration depth.

Acknowledgements

The results presented in this paper have been obtained within the frame of the SBO project IWT 03175 “Structural damage due to dynamic excitation: a multi-disciplinary approach”. This project is funded by IWT Vlaanderen, the Institute of the Promotion of Innovation by Science and Technology in Flanders. Their financial support is gratefully acknowledged.

References

[1] D. Aubry, D. Clouteau, A subdomain approach to dynamic soil-structure interaction, in: V. Davidovici, R.W. Clough (Eds.), Recent advances in Earthquake Engineering and Structural Dynamics, Ouest Editions/AFPS, Nantes, 1992, pp. 251–272.
[2] D. Clouteau, Propagation d'ondes dans des milieux hétérogènes. Application à la tenue des ouvrages sous séismes, Ph.D. Thesis, Ecole Centrale Paris, 1990.
[3] D. Clouteau, MISS Revision 6.2, Manuel Scientifique, 1999.
[4] A.J. Deeks, M.F. Randolph, Analytical modeling of hammer impact for pile driving, Internat. J. Numer. Anal. Methods Geomech. 17 (1993) 279–302.
[5] D.S. Kim, J.S. Lee, Propagation and attenuation characteristics of various ground vibrations, Internat. J. Soil Dynamics Earthquake Eng. 19 (2000) 115–126.
[6] L. Pyl, D. Clouteau, G. Degrande, A weakly singular boundary integral equation in elastodynamics for heterogeneous domains mitigating fictitious eigenfrequencies, Eng. Anal. Boundary Elem. 28 (2004) 1493–1513.
[7] F. Rausche, G. Goble, G. Likins, Investigation of dynamic soil resistance on piles using GRLWEAP, in: Proceedings of the Fourth International Conference on the Application of the Stress-Wave Theory to Piles, A.A. Balkema, Netherlands, 1992, pp. 137–142.
[8] J.F. Wiss, Construction vibrations: state of the art, ASCE J. Geotechnical Eng. Division 107 (GT2) (1981) 167–181.